UNSTRUCTURED NODAL DISCONTINUOUS GALERKIN SIMULATION OF SEISMC WAVE PROPAGATION IN HETEROGENEOUS SOLID MEDIA

Pranowo[1] and A. Gatot Bintoro[2]

We present a study of elastic wave propagation in heterogeneous media. The Discontinuous Galerkin Method is applied to solve the elastodynamic equations which represent seismic wave propagation. The elastodynamic equations are transformed into a stress-velocity formulation. The Discontinuous Galerkin Method is a finite element that allows a discontinuity of the numerical solution at element interface. Through a proper choice of the flux computation points, the method only requires communication between elements that have common faces. . The domains are discretized into unstructured straight-sided triangles that allow enhanced flexibility when dealing with complex geometries. The stress and velocity fields are expanded into a high-order polynomial spectral approximation over each triangular element. We use perfectly matched layer (PML) as absorbing boundary conditions. The utilization of high-order Jacobi polynomials as basis functions has been shown to be more efficient in reducing the numerical dispersion and numerical dissipation. Temporal discretization utilized explicit low-storage Runge Kutta 4th order method. We compare the numerical results to the available exact solutions and the comparison shows a good agreement.

Keyword: seismic wave propagation, discontinuous galerkin, perfectly matched layer.

1 Introduction

Simulation of seismic wave propagation played an important role in geophysics for imaging the structure of the earths interior and understanding the geodynamic phenomena. The elastodynamic equations has been used intensively to model the seismic wave propagation in the earths. Because of analytical solutions of the equations are rare, the equations are solved numerically. The chalenge is to develop high performance numerical methods that are capable of solving the elastodynamic equations accurately and that can deal with complicated computational domain (Komatitsch & Villote ,1998)

Continuous efforts have been devoted for developing numerical methods. During the last two decades, finite-difference time-domain (FDTD) methods have used extensively in modeling a large variety seismic wave propagation problems (Virieux, 1986). FDTD methods directly simulate the physical systems by making discrete approximation for the time and spatial derivatives via Taylor expansion to turn the partial differential equations into a system of algebraic equations. This methods compute wavefields that are staggered in space and time and can be interpreted as standard leapfrog method. The FDTD methods suffer from poor numerical dispersion, which makes it difficult to run simulation for long time without introducing excessive errors and they have only second order accuracy in time and space. Some new schemes have also started with FDTD scheme but were extended for greater accuracy rather than for geometry. High-order staggered finite-difference schemes, including compact schemes, are developed to improve the FDTD's accuracy. Pranowo et al. (2003) developed multiresolution time-domain (MRTD) methods to simulate elastic wave fields. In the MRTD methods, the field components are expanded by using scaling and wavelet function then tested with using scaling and wavelet function through Galerkin's procedure. They show that computational effort can be reduced via wavelet thresholding. It is found that the implementation of MRTD on the boundaries is not easy task.

[1] Department of Informatics, Atma Jaya Yogyakarta University, Jl. Babarsari 43 Yogyakarta 55281 Indonesia.
[2] Department of Industrial Engineering, , Atma Jaya Yogyakarta University, Jl. Babarsari 43 Yogyakarta 55281 Indonesia.

Finite volume methods (FVM), intensively used to solve fluid dynamics problems, have been adopted for elastodynamic equations (Dormy & Tarantola, 1996). Le Veque (2004) calculated the flux of the wavefields based Riemann solver succesfuly. Contrary to the FDTD methods, the FV methods allow one to deal with complicated geometries. The FV methods have second order accuracy and it is difficult to increase the order accuracy.

Finite element methods (FEM), based on variational formulation, can handle complicated geometries and heterogeneous material properties easily. The FE method exhibit poor dispersion properties for simulating wave propagation. Komatistsch & Vilotte (1998) used Spectral element methods (SEM) simulating seismic wave propagation. SEM are high-order Finite element methods which solve the variational formulations of the equations using spectral functions as basis functions. The Spectral element methods generate large global matrix from the elemental matrix, the methods require too much computer memory and CPU time. Recently, Discontinuous Galerkin (DG) methods (Pranowo et al., 2004; Dumbser & Kaser, 2006) have been developed to overcome the dispersion problems.

In this paper, elastodynamic equations, which described sesismic wave propagation, are solved using DG method. High order Jacobi polynomials are used as basis functions. The elastodynamic equations will be discretized using triangular mesh and explicit low-storage Runge-Kutta 4th method is used as time integration method.

2 Elastodynamic Equations

Our approach of treating seismic waves numerically is based on the theory elastodynamics. We use the velocity-stress formulation as the governing equations:

$$
\begin{aligned}
&\frac{\partial v_x}{\partial t} = \frac{1}{\rho}\left(\frac{\partial \tau_{xx}}{\partial x} + \frac{\partial \tau_{xy}}{\partial y}\right) + f_x \quad ; \quad \frac{\partial v_y}{\partial t} = \frac{1}{\rho}\left(\frac{\partial \tau_{xy}}{\partial x} + \frac{\partial \tau_{yy}}{\partial y}\right) + f_y \\
&\frac{\partial \tau_{xx}}{\partial t} = (\lambda + 2\mu)\frac{\partial v_x}{\partial y} + \lambda\frac{\partial v_y}{\partial x} \quad ; \quad \frac{\partial \tau_{yy}}{\partial t} = \lambda\frac{\partial v_x}{\partial y} + (\lambda + 2\mu)\frac{\partial v_y}{\partial x} \\
&\frac{\partial \tau_{xy}}{\partial t} = \mu\left(\frac{\partial v_y}{\partial x} + \frac{\partial v_x}{\partial y}\right)
\end{aligned}
\tag{1}
$$

In which v_x and v_y are the components of the velocity vector, τ_{xx}, τ_{yy} and τ_{xy} are the elements of the stress tensor and (f_x, f_y) is body force vector. The medium is isotropic and described by the density $\rho(x,y)$ and the Lame coefficients $\lambda(x,y)$ and $\mu(x,y)$.

3 Discontinuous galerkin methods

The spatial derivatives are discretized by using a discontinuous galerkin method. The simplified of Eq.(1) according to Galerkin's procedure using the same basis function ϕ within each element is defined below (Hesthaven & Warburton, 2002; 2004; 2008):

$$\left(\phi, \frac{\partial \mathbf{q}}{\partial t} + \mathbf{A}\frac{\partial \mathrm{q}}{\partial x} + \mathbf{B}\frac{\partial \mathrm{q}}{\partial y}\right) = 0$$

$$\Leftrightarrow \left(\phi, \frac{\partial \mathrm{q}}{\partial t}\right)_{\Omega} + \left(\phi, \mathbf{A}n_x\mathbf{q} + Bn_y\,\mathrm{q}\right)_{\partial\Omega} - \left(\frac{\partial}{\partial x}(\mathbf{A}\phi), \mathrm{q}\right) - \left(\frac{\partial}{\partial y}(\mathbf{B}\phi), \mathbf{q}\right)_{\Omega} = 0 \tag{2}$$

Here $(.,.)$ represents the normal L_2 inner product, the second term is flux vector and (n_x, n_y) are normal vector. The mathematical manipulation of the flux vector is as below:

$$\left(\phi, \frac{\partial \mathrm{q}}{\partial t} + \mathbf{A}\frac{\partial \mathrm{q}}{\partial x} + \mathbf{B}\frac{\partial \mathrm{q}}{\partial y}\right)_{\Omega} + \left(\phi, \mathbf{A}n_x + \mathbf{B}n_y\right)\left(\hat{\mathrm{q}} - \mathrm{q}^-\right)_{\partial\Omega} = 0 \tag{3}$$

where,

$$\hat{\mathbf{q}}\big|_{\partial\Omega} = \hat{\mathbf{q}}^-\left(\mathbf{q}^-, \mathbf{q}^+\right)\Big|_{\partial\Omega}$$

In this problem, the numerical flux vector is calculated by using central flux.

$$\hat{\mathbf{q}}\big|_{\partial\Omega} = 0.5\left(\mathbf{q}^- + \mathbf{q}^+\right)\Big|_{\partial\Omega} \tag{4}$$

Here, we took the Kornwinder Dubiner function on straight sided triangle as the basis written in equation 5 (see Figs. 1 and 2):

$$\phi_{ij}(r,s) = \sqrt{\frac{2i+1}{2}}\sqrt{\frac{2i+2j+2}{2}}P_i^{0,0}\left(\frac{2(1+r)}{(1-s)} - 1\right)P_j^{2=+1,0}(s) \tag{5}$$

where, $P^{\alpha,\beta}$ is orthogonal Jacobi polynomial

All straight sided triangles are the image of this triangle under the map:

$$\begin{pmatrix} x \\ y \end{pmatrix} = -\left(\frac{r+s}{2}\right)\begin{pmatrix} v_x^1 \\ v_y^1 \end{pmatrix} + \left(\frac{1+r}{2}\right)\begin{pmatrix} v_x^2 \\ v_y^2 \end{pmatrix} + \left(\frac{1+s}{2}\right)\begin{pmatrix} v_x^3 \\ v_y^3 \end{pmatrix} \tag{6}$$

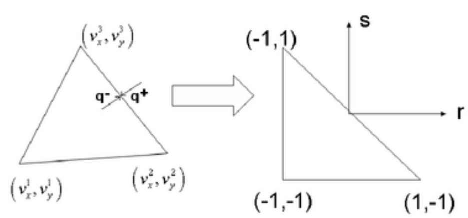

Figure 1.
Coordinate Transformation

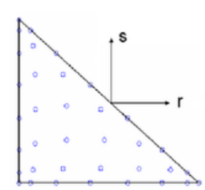

Figure 2.
Seventh order Gauss Lobatto Quadrature Nodes

The vector $\mathbf{q} = (\tau_{xx} \quad \tau_{xy} \quad \tau_{yy} \quad v_x \quad v_y)^T$ is expanded using equation (5), we take expansion of v_x as example:

$$v_x(r,s) = \sum_{i=0}^{N}\sum_{j=0}^{N-i}\phi_{ij}(r,s)\hat{v}_{xij} \tag{7}$$

$$v_x(r_n,s_n) = \sum_{m=1}^{m=M}\mathbf{V}_{nm}\hat{v}_{xm} \Rightarrow \hat{v}_{xm} = \sum_{m=1}^{m=M}(\mathbf{V}^{-1})_{mj}v_x(r_j,s_j) \tag{8}$$

$$\begin{aligned}\frac{\partial v_x}{\partial r}(r,s) &= \sum_{i=0}^{N}\sum_{j=0}^{N-i}\frac{\partial \phi_{ij}}{\partial r}(r,s)\hat{v}_{xij} = \hat{\mathrm{D}}^r\mathbf{V}^{-1}v_x(r,s)\\ \frac{\partial v_x}{\partial s}(r,s) &= \sum_{i=0}^{N}\sum_{j=0}^{N-i}\frac{\partial \phi_{ij}}{\partial s}(r,s)\hat{v}_{xij} = \hat{\mathrm{D}}^s\mathbf{V}^{-1}v_x(r,s)\end{aligned} \quad ; \ \hat{\mathbf{D}}^r = \frac{\partial \phi}{\partial r} \ ; \ \hat{\mathbf{D}}^s = \frac{\partial \phi}{\partial s} \tag{9}$$

where $\mathbf{V}_{ij}$ and N are Vandermonde matrix dan the order of Jacobi polynomial respectively.

The semi discrete Eq. (3) is integrated in time marching by using five stages of fourth order 2N-storage Runge-Kutta scheme as developed by Carpenter & Kennedy (1994). The final equations are found as written in Eqs. (10) and (11) and the 5-stage of 2N-storage Runge-Kutta algorithm respectively.

$$\frac{d\mathbf{q}}{dt} = L[t,\mathbf{q}(t)] \tag{10}$$

$$\begin{aligned} d\mathbf{q}_j &= A_j d\mathbf{q}_{j-1} + dtL(\mathbf{q}_j)\\ \mathbf{q}_j &= \mathbf{q}_{j-1} + B_j + d\mathbf{q}_j \end{aligned} \tag{11}$$

where dt is the time step. The vectors A and B are the coefficients that will be used to determine the properties of the scheme. The maximum time step is (Hesthaven and Warburton, 2001):

$$\Delta t \le \frac{2h}{C_p(N-1)^2} \tag{12}$$

where C_p is primary wave velocity and h is the smallest edge length of the element.

4 PML absorbing boundary condition

The Simulation osf seismic waves by discontinuous galerkin methods in unbounded domains requires a specific boundary condition of the necessarily truncated computational domain. In theis paper we propose an absorbing boundary condition called perfectly matched layer (PML). The Elastodynamic Equations (eq.1) are split with respect to spatial coordinates for PML absorbing boundary conditions and one dimensional damping functions (σ_x, σ_y) are applied to the split wavefields.

$$
\begin{aligned}
&\frac{\partial v_{xx}}{\partial t}+\sigma(x)v_{xx}=\frac{1}{\rho}\frac{\partial \tau_{xx}}{\partial x}+f_x &;\quad &\frac{\partial v_{xy}}{\partial t}+\sigma(y)v_{xy}=\frac{1}{\rho}\frac{\partial \tau_{xy}}{\partial y}\\
&\frac{\partial v_{yx}}{\partial t}+\sigma(x)v_{yx}=\frac{1}{\rho}\frac{\partial \tau_{xy}}{\partial x} &;\quad &\frac{\partial v_{yy}}{\partial t}+\sigma(y)v_{yy}=\frac{1}{\rho}\frac{\partial \tau_{yy}}{\partial y}+f_y\\
&\frac{\partial \tau_{xxx}}{\partial t}+\sigma(x)\tau_{xxx}=(\lambda+2\mu)\frac{\partial v_x}{\partial y} &;\quad &\frac{\partial \tau_{xxy}}{\partial t}+\sigma(y)\tau_{xxy}=\lambda\frac{\partial v_y}{\partial x}\\
&\frac{\partial \tau_{yyx}}{\partial t}+\sigma(x)\tau_{yyx}=\lambda\frac{\partial v_x}{\partial y} &;\quad &\frac{\partial \tau_{yyy}}{\partial t}+\sigma(y)\tau_{yyy}=(\lambda+2\mu)\frac{\partial v_y}{\partial x}\\
&\frac{\partial \tau_{xyx}}{\partial t}+\sigma(x)v_{xyx}=\mu\frac{\partial v_y}{\partial x} &;\quad &\frac{\partial \tau_{xyy}}{\partial t}+\sigma(y)v_{xyy}=\mu\frac{\partial v_x}{\partial y}
\end{aligned}
\qquad (13)
$$

where $v_x = v_{xx} + v_{xy}$, $v_y = v_{yx} + v_{yy}$, $\tau_{xx} = \tau_{xxx} + \tau_{xxy}$, $\tau_{yy} = \tau_{yyx} + \tau_{yyy}$, $\tau_{xy} = \tau_{xyx} + \tau_{xyy}$

5 Numerical results and discussion

5.1 Exact solution

We consider a problem defined on the unit square $(0,1)\times(0,1)$ wih $(v_x, v_y)=0$ on the boundary. We choose the body force and exact solutions as (Li, 1996):

$$
\begin{aligned}
f_x &= (\lambda+\mu)(1-2x)(1-2y)Sin\omega t\\
f_y &= (\rho\omega^2 xy(1-x)(1-y) - 2\mu y(1-y) \text{-} 2(\lambda+2\mu)x(1-x))Sin\omega t \qquad (14)\\
v_y &= -xy(1-x)(1-y)Cos\omega t
\end{aligned}
$$

Plain strain condition is assumed and the parameters are taken as E = 1.0, ν = 0.3, ρ = 1.0, ω = π, time step = 0.01, numbers of element = 16 and polynomial order varies from N = 3. Comparisons with the exact solutions are shown in figure 3 for v_y profile, very good agreements are found. Figure 4 shows that trends of DG maximum errors almost constant in time, the growth of error (dispersive & dissipation error) in DG method can be reduced by using high-order basis

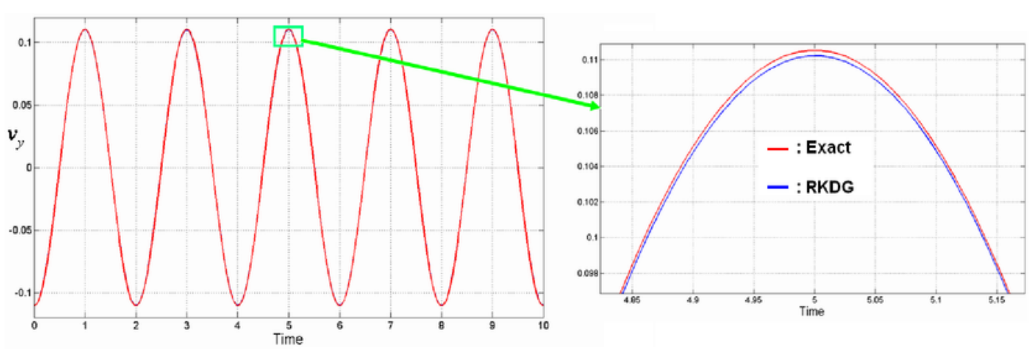

Figure 3.
Histories of v_y responses at the point (0.25,0.25).

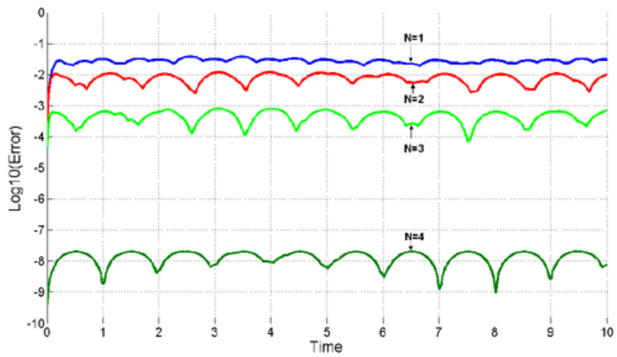

Figure 4.
Histories of $\left|(v_y)_{RKDG} - (v_y)_{exact}\right|_\infty$ maximum errors of v_y.

5.2 Simulation with free surface topography

The model we consider is two layered elastic half-space with prescribed topography. The medium has a horizontal internal boundary that divides it into two layers. The upper layer is characterized by a *P*-wave velocity of 2600 m.s^{-1}, an *S*-wave velocity of 1400 m.s^{-1}, and a mass density of 2200 kg.m^{-2}. The lower layer elastic parameters are a *P*-wave velocity of 5500 m.s^{-1}, an *S*-wave velocity of 3200 m.s^{-1}, and a mass density of 2500 kg.m^{-2}. A strong contrast both in velocity is hence modeled. inside the upper layer. The domain has width of 3200 m and average height of 2700 m. The line of receivers goes from x = 1500 m to x = 2500 m at y = 2500 m. The source is gaussian function in space and dirac delta in time and the position is (x,y) = (2000,1200). The time step is $\Delta t = 0.25\,\mathrm{m\,sec}$. PML absorbing boundaries are used on left, right and bottom edges and free stress is used on top edge of the domain. The mesh of the domain, including PML, is composed of 6489 triangular elements.

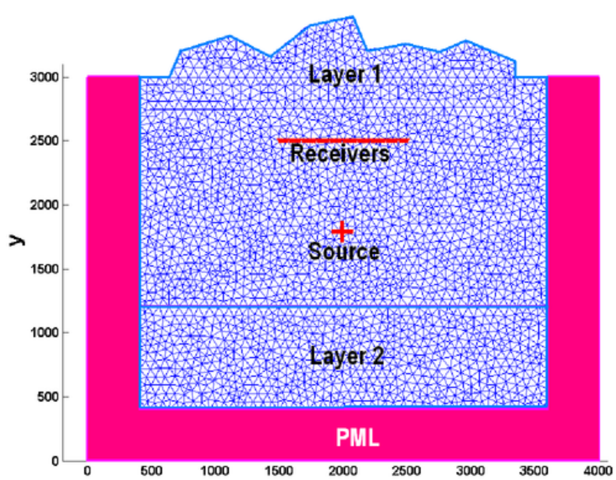

Figure 5. Two layered heterogeneous elastic media

Figure 6 shows the snapshots of $P-SV$ wave propagation in two-layered media at $t=0.2, t=0.3, t=0.4, t=0.5, t=0.7$, and $t=0.8$s . The entire wavefields are composed of direct phases *(P,S)*, reflected waves from internal boundary *(PPr, PSr,SPr, SSr)* or the free surface *(PP,PS)*. Mode conversions of wave reflected at the internal boundary as well as at the top free surface are clearly visible. From figure 6c. 6d, 6e and 6f we can see no reflection on the left, right and bottom edges. The PML absorbed outgoing waves well.

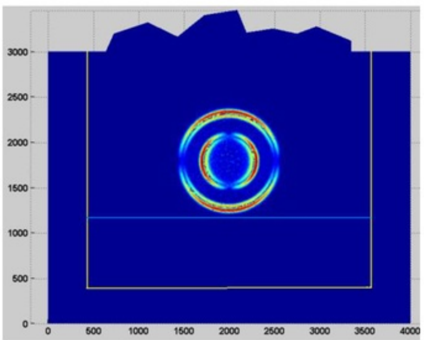

Figure 6a. v_y field at $t=0.2$ s

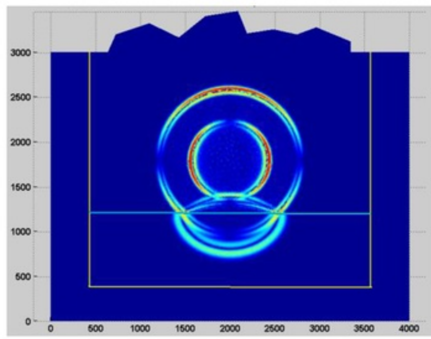

Figure 6b. v_y field at $t=0.3$ s

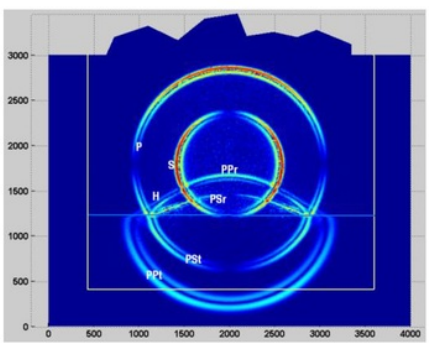

Figure 6c. v_y field at $t=0.4$ s

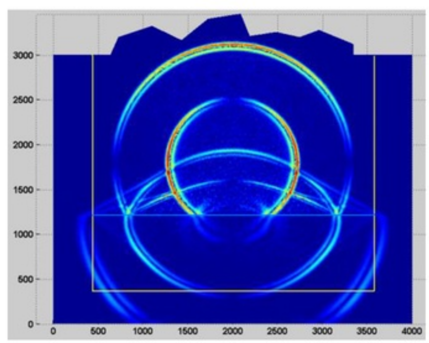

Figure 6d. v_y field at $t=0.5$ s

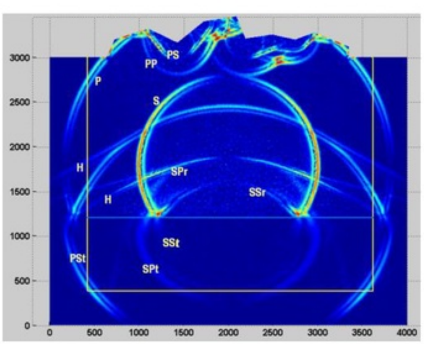

Figure 6e. v_y field at $t=0.7$ s

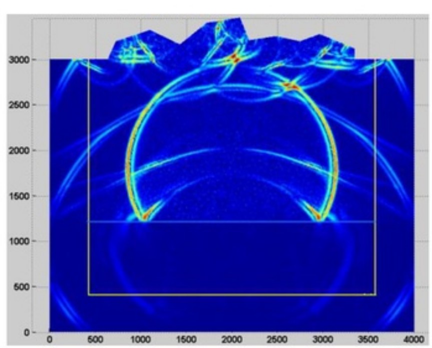

Figure 6f. v_y field at $t=0.8$ s

Figure 7 shows the numerical time response of $P-SV$ waves in heterogeneous medium recorded at 51 receivers placed horizontally inside the medium.

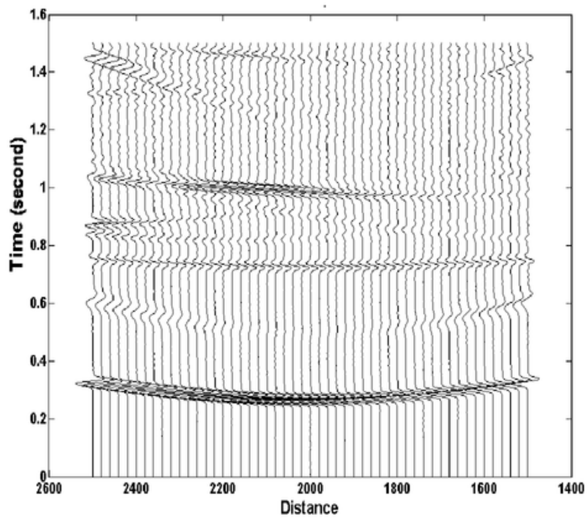

Figure 7. Seismogram of v_y

6 Conclusion

We have presented high-order discontinuous galerkin method on unstructured mesh for simulation of seismic wave propagation in complex medium. We demonstrated that DG method can handle irregular heterogeneous domain easily. Wave phenomena, such as: mode conversion, transmission and reflection can be captured well. We found good qualitative agreement with exact solution. Future work will focus on applying the method to more realistic structures, for instance regions with fault zones.

Acknowledgment

We are very grateful to Prof. Hesthaven and Dr. Tim Warburton for the valuable discussion and providing their Useme Matlab code. This research is supported by Indonesia Toray Scientific Foundation.

References

Carpenter M. H. and Kennedy C. A., 1994, *Fourth-order 2N-Storage Runge-Kutta Schemes,* NASA Technical Memorandum 109112, NASA Langley Research Center, Hampton, Virginia.

Dormy, E. & A. Tarantola (1996), *Numerical simulation of elastic wave propagation using a finite volume method*, J. Geophysics. Res., 100, 2123-2133.

Hesthaven, J. S. and Warburton, T., 2002, *High-order Nodal Methods on Unstructured Grids, I. Time Domain Solution of Maxwell's Equations*, J. Computational Physics, 181, pp. 1-34.

Hesthaven, J. S. and Warburton, T., 2004, *High-order Nodal Discontinuous Galerkin Methods for Maxwell Eigen Value Problem,* Philosophical Transactions of The Royal Society of London, Series A, Mathematical and Physical Sciences, 362 (1816): 493-524.

Hesthaven, J. S. and Warburton, T., 2008, *Nodal Discontinuous Galerkin Methods: Algorithms, Analysis, and Applications*, Springer, New York.

Kaser, Martin. And Dumbser, Michael, 2005, *An Arbitrary High Order Discontinuous Galerkin for Elastic Wave on Unstructured Meshes I: The Two Dimensional Isotropic Case*, Spice Report.

Komatitsch, D. & J. P.Villote, 1998, *The spectral element Method: An efficient tool to simulate response of 2D and 3D geological structure, Bulletin of the Seismological Society of America*, Vol. 2, 368-392.

Le Veque, R.J. (2004), *Finite-Volume methods for hyperbolic problems*, University Press, Cambridge.

Pranowo, F. Soesianto & B. Y. Andiyanto (2003), The Multiresolution time-domain method based on Haar wavelets for numerical simulation of elastic wave propagation, *Proceedings of Inte*

T1

ORIGINALITY REPORT

19%	14%	19%	9%
SIMILARITY INDEX	INTERNET SOURCES	PUBLICATIONS	STUDENT PAPERS

PRIMARY SOURCES

1	Pranowo Pranowo, Djoko Budiyanto Setyohadi. "Numerical simulation of electromagnetic radiation using high-order discontinuous galerkin time domain method", International Journal of Electrical and Computer Engineering (IJECE), 2019 Publication	3%
2	David Michéa, Dimitri Komatitsch. "Accelerating a three-dimensional finite-difference wave propagation code using GPU graphics cards", Geophysical Journal International, 2010 Publication	2%
3	seismic.yonsei.ac.kr Internet Source	2%
4	X.D. Li, N.-E. Wiberg. "Implementation and adaptivity of a space-time finite element method for structural dynamics", Computer Methods in Applied Mechanics and Engineering, 1998 Publication	2%
5	www.mfo.de Internet Source	

1%

6 authors.library.caltech.edu
Internet Source
1%

7 www.caam.rice.edu
Internet Source
1%

8 Submitted to Imperial College of Science, Technology and Medicine
Student Paper
1%

9 repositories.lib.utexas.edu
Internet Source
1%

10 Stanescu, D.. "Aircraft engine noise scattering by fuselage and wings: a computational approach", Journal of Sound and Vibration, 20030529
Publication
1%

11 Michael Dumbser. "An arbitrary high-order discontinuous Galerkin method for elastic waves on unstructured meshes ? II. The three-dimensional isotropic case", Geophysical Journal International, 10/2006
Publication
1%

12 www.agu.org
Internet Source
1%

13 E. D. Mercerat. "Triangular Spectral Element

simulation of two-dimensional elastic wave propagation using unstructured triangular grids", Geophysical Journal International, 8/2006
Publication | 1%

14 www.gps.caltech.edu
Internet Source | 1%

15 link.springer.com
Internet Source | 1%

16 www.mdpi.com
Internet Source | 1%

17 International Journal of Numerical Methods for Heat & Fluid Flow, Volume 23, Issue 1 (2013-01-05)
Publication | 1%

18 Ursula Iturraran-Viveros. "Scattering of elastic waves in heterogeneous media using the direct solution method", Geophysical Journal International, 2/2004
Publication | 1%

Exclude quotes Off
Exclude bibliography Off
Exclude matches < 1%

T1

GRADEMARK REPORT

FINAL GRADE

/0

GENERAL COMMENTS

Instructor

PAGE 1

PAGE 2

PAGE 3

PAGE 4

PAGE 5

PAGE 6

PAGE 7

PAGE 8

PAGE 9